

Signature of a crossed Andreev reflection effect in the magnetic response of $\text{YBa}_2\text{Cu}_3\text{O}_{7-\delta}$ junctions with the itinerant ferromagnet SrRuO_3

P. Aronov and G. Koren*

Physics Department, Technion, Israel Institute of Technology Haifa, 32000, Israel

(Received 6 June 2005; revised manuscript received 3 October 2005; published 22 November 2005)

The magnetic properties of superconducting-ferromagnetic-superconducting (SFS) and SF ramp-type junctions with $\text{YBa}_2\text{Cu}_3\text{O}_{7-\delta}$ (YBCO) electrodes (S) and the itinerant ferromagnet SrRuO_3 (SRO-F), were investigated. We looked for a crossed Andreev reflection effect (CARE) in which an electron from one magnetic domain in F is Andreev reflected as a hole into an adjacent, oppositely polarized, domain while a pair is transmitted into S. The CARE is possible in SRO since the width of its domain walls is of the order of the YBCO coherence length (2–3 nm). Our junctions behave as typical magnetic tunneling junctions, as the conductance spectra were always asymmetric and a few showed bound-state peaks at finite bias that shifted with field according to classical Tedrow-Meservey theory. In many of our SFS junctions with a barrier thickness of 10–20 nm, a prominent zero-bias conductance peak (ZBCP) has been observed. This peak was found to decrease *linearly* with magnetic field, as expected for Andreev and CARE scattering. In contrast, in SF junctions, the observed ZBCP was found to decrease versus field almost *exponentially*, in agreement with the Anderson-Appelbaum theory of scattering by magnetic states in F. Thus, transport in our SFS and SF junctions depends strongly on the size of the F layer. We also found that in both cases, the ZBCP height at zero field decreased with increasing magnetic order of the domains in F, in agreement with the CARE mechanism.

DOI: [10.1103/PhysRevB.72.184515](https://doi.org/10.1103/PhysRevB.72.184515)

PACS number(s): 74.45.+c, 75.70.-i, 74.50.+r, 74.78.Bz

The properties of superconducting-ferromagnetic-superconducting (SFS) ramp-type junctions of $\text{YBa}_2\text{Cu}_3\text{O}_{7-\delta}$ (YBCO) electrodes (S) and SrRuO_3 (SRO) barriers (F) were investigated by two groups more than ten years ago.^{1,2} Both groups found that the normal resistance values of their junctions show two distinct phenomena. One is that the observed values had a large spread from a few tens of ohms to a few hundred ohms, and the other is that they were two or more orders of magnitude higher than the expected Ohmic resistance of the SRO film. The high normal resistance was therefore assumed to originate at the YBCO/SRO interfaces and more specifically attributed to oxygen disorder and depletion near the interfaces.^{2–4} Dömel *et al.* attributed the high normal resistance to an insulating interface layer through which quasiparticle tunneling via localized states occurred.² A second explanation to the high normal resistance was given by Antognazza *et al.* who attributed it to interface stress created by thermal expansion mismatch in the junctions.¹ Conductance spectra of YBCO-based SFS junctions with SRO and CaRuO_3 (CRO) barriers were also measured by Antognazza *et al.*⁵ With both type of barriers they found a zero-bias conductance peak (ZBCP) in the center of a tunnelinglike gap structure. The critical current density, however, in the junctions with the CRO barrier persisted up to a barrier thickness of 50 nm, while that of the junctions with the SRO barrier vanished abruptly already at a thickness of 25 nm.^{3,6} Since SRO is an itinerant ferromagnet below ~ 150 K,^{7,8} while CRO is a paramagnet, the different behavior of the critical current density indicates that the magnetic properties of the barrier layer play an important role in the transport of these junctions.

In the present study we reexamine the same type of junctions of YBCO and SRO, with a special focus on transport properties which are affected by the magnetic nature of the

barrier material. In the absence of a critical current, transport in junctions at voltage bias values below the energy gap of the superconductor is controlled by Andreev scattering. When the barrier material is fully spin polarized in one direction, no Andreev transport is possible. If, however, the ferromagnetic barrier has many domains with opposite polarizations, a crossed Andreev reflection effect (CARE) is possible.⁹ This effect can occur at the intersection of the domain walls and the YBCO electrodes at the interfaces, provided the value of the domain wall width is similar to that of the superconductor's coherence length ξ (2–3 nm for optimally doped YBCO). We have chosen to study junctions with an SRO barrier since the domain wall width of this highly anisotropic ferromagnet is very narrow (~ 3 nm only^{10,11}) and fulfills the above condition. As will be described in the following, our conductance spectrum results under magnetic fields provide supportive evidence for the existence of the CARE in our junctions. It should be noted that recently the CARE was observed by Beckmann *et al.* in conventional FSF junctions made of two closely spaced Fe nanowires in contact with an Al electrode.¹² They found that the resistance difference between parallel and antiparallel magnetization of the Fe electrodes when the Al electrode was in the superconducting state decays with increasing distance of the Fe electrodes up to about one coherence length of Al, in agreement with the CARE phenomenon. Technically, however, it is impossible to reproduce this kind of study in the high-temperature superconductors due to their extremely short coherence length.

We prepared the YBCO-based ramp-type junctions with SRO on (100) SrTiO_3 (STO) wafers with a ramp angle of $\sim 35^\circ$. This was done by a multistep process, where the epitaxial thin-film layers are prepared by laser ablation deposition, patterning is done by deep UV photolithography, and

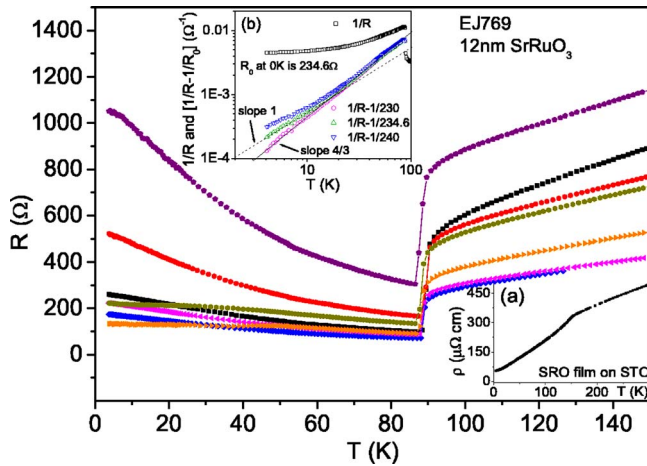


FIG. 1. (Color online) Resistance versus temperature of several junctions on a single wafer. Inset (a): resistivity versus temperature of a 90-nm-thick SrRuO₃ film on (100) STO. Inset (b): inverse resistivity of one of the low-resistance junctions (*J*₆—see the inset of Fig. 2) versus *T* on a log-log scale (solid line, $T^{4/3}$ slope; dashed line, T^1 slope).

etching by Ar ion milling.¹³ The YBCO films had *c*-axis orientation normal to the wafer. The thickness of the base and cover electrodes was kept constant at 80 nm, while the SRO thickness on different wafers ranged between 4 and 45 nm. On each wafer we patterned ten identical junctions along the (100) direction, with a width of 5 μm. Finally, a gold layer was deposited and patterned to produce the 4 × 10 contact pads for the four-probe transport measurements. The YBCO electrodes of our junctions had oxygen content close to optimal doping with a T_c of 88–89 K. The quality of our junctions fabrication process was tested by measuring the critical current density J_c of “shorts” (junctions without any barrier). We found $J_c(77\text{ K}) \sim 1 \times 10^6\text{ A/cm}^2$, which is reasonable compared to $J_c(77\text{ K}) \sim 3\text{--}5 \times 10^6\text{ A/cm}^2$ found in the best blanket films.

Figure 1 shows the resistance versus temperature of several junctions on a single wafer. The spread of resistance values at temperatures above T_c is *extrinsic* and due to the different lengths of the YBCO leads to the junctions. At low temperatures, the resistance values have an *intrinsic* large spread of about one order of magnitude. These resistance values are also several order of magnitude higher than the calculated 10-mΩ Ohmic resistance of the junction obtained by using the resistivity of the SrRuO₃ film [see inset (a) to Fig. 1]. These observations are similar to the results reported previously on the same kind of junctions by other groups as discussed at the beginning of this paper.^{1,2} Unlike previous results, however, our junctions generally had a critical current up to a barrier thicknesses of ~10 nm, but were resistive at higher barrier thicknesses. Antognazza *et al.* found critical currents with a barrier thickness of up to 25 nm.¹ This is possibly due to microshorts or tunneling via oxygen disorder states in their junctions. Dömel *et al.* have found that the inverse resistance difference $1/R - 1/R_0$ of their junctions (where R_0 is the extrapolated resistance to $T=0$) varies versus temperature as $T^{4/3}$. They concluded that this indicates tunneling via one and two localized states in the barrier.^{2,14}

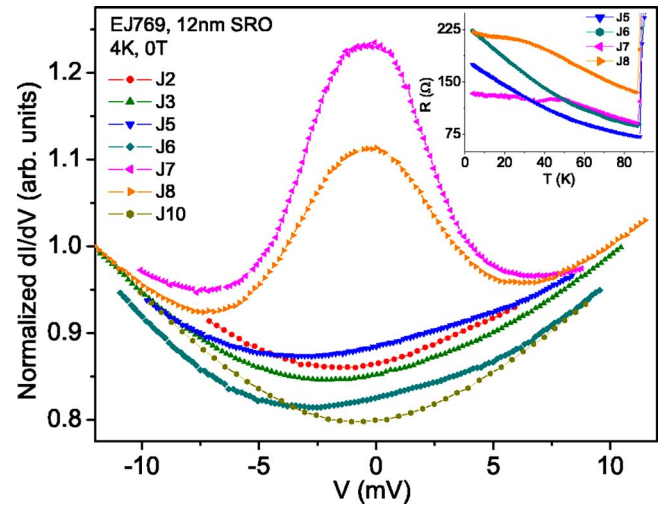


FIG. 2. (Color online) Normalized conductance spectra of several junctions on a single wafer. Inset: blowup of the resistance versus temperature of a few junctions.

We basically observed a similar behavior as shown in inset (b) to Fig. 1. As one can see, however, the results are very sensitive to R_0 and the $T^{4/3}$ behavior is not obtained with the extrapolated R_0 , but a value close to it. Furthermore, in the study of Dömel *et al.* there are no data between 5 and 20 K. If we use our data in this temperature range and with the extrapolated R_0 value, we find a *linear* dependence versus T . Thus we believe that tunneling via two localized states is *not* the dominant transport mechanism in our junctions.

Figure 2 shows the normalized conductance spectra at low temperature of several junctions on a single wafer with a barrier thickness of 12 nm. One observes that two junctions have a ZBCP inside a tunnelinglike structure, while the others have only tunnelinglike behavior. This ZBCP can be attributed to Andreev reflections but also to scattering by magnetic states.^{15–17} Since our junctions are orientated along the *a* or *b* axis of the YBCO electrodes, in principle, one should not expect any ZBCP due to Andreev bound states (ABS's) as calculated by Tanaka *et al.* in NS junctions.^{18,19} We note that the maximal alignment deviation of our junctions from the (100) direction is of about 2°, but this is too small to give rise to a significant ZBCP due to ABS's. However, the intrinsic roughness of the interface in our junctions, of the order of 1 nm,²⁰ could give rise to a ZBCP of ABS origin.²¹ In addition, we point out that there is a correlation between the appearance of a ZBCP and the behavior of the resistance curves below T_c (see the inset to Fig. 2). For junction *J*₇ and *J*₈, where a ZBCP was observed, the *R* versus *T* curves show a change of slope (a cusp) and not a monotonic increase with decreasing temperature as for instance is found in junctions *J*₅ and *J*₆. Another distinct feature in Fig. 2 is that the spectra are clearly asymmetric. This asymmetry is typical of ferromagnetic tunneling junctions due to the opposite shifts of the spectra for up and down spins, and the non zero-spin polarization of the magnetic electrode.²² Further support for the fact that our junctions behave as classical magnetic tunneling junctions is found in Fig. 3. In this figure one sees the prominent ZBCP and its suppression under applied magnetic

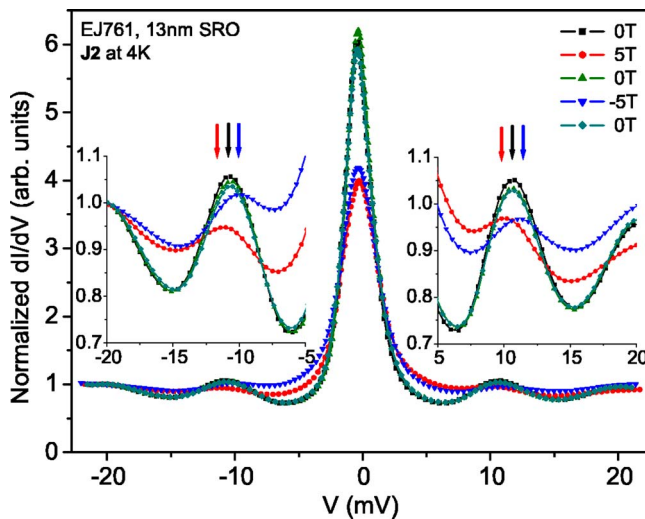


FIG. 3. (Color online) Normalized conductance spectra of a junction under zero-field cooling (ZFC) to 4 K followed by field cycling to 5 T, 0 T, -5 T and back to 0 T. Insets: zoom up on the spectra of the bound states near 10 and -10 mV.

fields. But first we shall focus on the bound-state peaks observed at about ± 10 mV. As can be seen by the blowup of these parts of the spectra, a positive magnetic field shifts the peak to negative bias and vice versa (hole carriers). The total measured shift for fields of ± 5 T is ~ 1.2 mV. The expected shift for an SFS junction is $4\mu H$ (1.28 mV here).²² Thus for a bound state of energy Δ_1 , the expected shift $4\mu H/2\Delta_1$ should be equal to the measured shift $\sim 1.2/\Delta$ where Δ is the gap energy. Therefore, $2\Delta_1 \sim \Delta$, and if Δ of YBCO is ~ 20 meV, then $\Delta_1 \sim 10$ meV, in agreement with the peaks bias of the bound state in Fig. 3.

Figure 4 shows a few conductance spectra under different fields and field cooling conditions. There is almost no effect on the spectra at any given field larger than about 0.1 T,

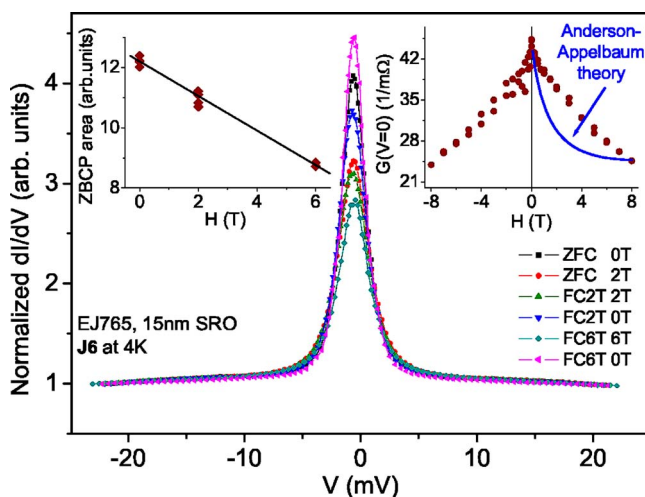


FIG. 4. (Color online) Normalized conductance spectra under various fields and field cooling conditions to 4 K. Insets: the conductance peak area and the conductance at zero bias versus field. The solid curve is a typical theoretical prediction of the Anderson-Appelbaum model.

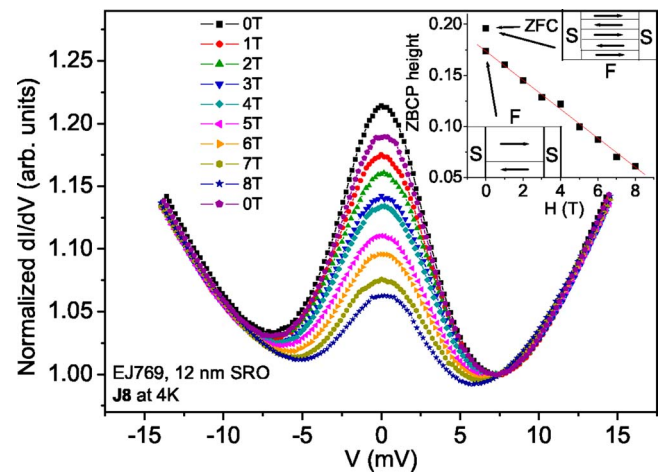


FIG. 5. (Color online) Normalized conductance spectra under ZFC to 4 K, followed by field ramping to 8 T and back to 0 T. Inset: the ZBCP height above the background conductance $G_0 - G_B$ versus field. G_B was taken as the conductance value at $V=0$ of the straight line connecting the two minima of each spectrum.

whether it was obtained under zero-field cooling (ZFC) or field cooling (FC). The insets of Fig. 4 show the ZBCP area above the background conductance and the conductance at zero bias [$G_0 \equiv G(V=0) = 1/R(V=0)$] versus field. Surprisingly, both features show a *linear* decrease with increasing field, except maybe for fields near zero field. The conductance G_0 versus field due to scattering by magnetic states in junctions was calculated by Appelbaum and found to be almost exponential.²³ A similar behavior, but with a more gradual decrease versus field, was found also in experiments done in Ta-I-Al tunnel junctions.²⁴ Thus the observed linear G_0 versus H result in our junctions may be indicative of a different scattering mechanism, possibly ABS's due to interface roughness.²¹ A theoretical calculation of the current and magnetoresistance in FSF junctions due to the CARE was recently published,²⁵ but it did not include conductance spectra which are relevant in the present study. The closest theoretical calculation we could find for a ZBCP behavior versus H was in studies by Tanaka *et al.*^{18,19} Extracting G_0 from their conductance spectra of Fig. 1(b) of Ref. 18 (node direction) at different fields, one finds a clear linear decrease with field. Since our data are consistent with this behavior, it is likely that local Andreev and nonlocal CARE processes play a dominant role in the transport of our SFS junctions.

Figure 5 shows a series of conductance spectra in another junction. These spectra were obtained under various fields starting with ZFC to 4 K, ramping up to 8 T, and going back to zero field. Here, again as in Fig. 4, one finds a linear decrease of the ZBCP height versus field as shown in the inset to this figure, but the ZFC datum point seems to stand out. Clearly, the measured ZBCP height after ZFC is larger than that obtained after field cycling to 8 T and back to 0 T. To understand this behavior, we note that during the ZFC process, the SRO barrier layer becomes ferromagnetic with many domains and domain walls as shown schematically in the upper-right corner of the inset. As a result, the contribution of the CARE to the conductance, which depends on the number of domain wall intersections with the S electrodes,

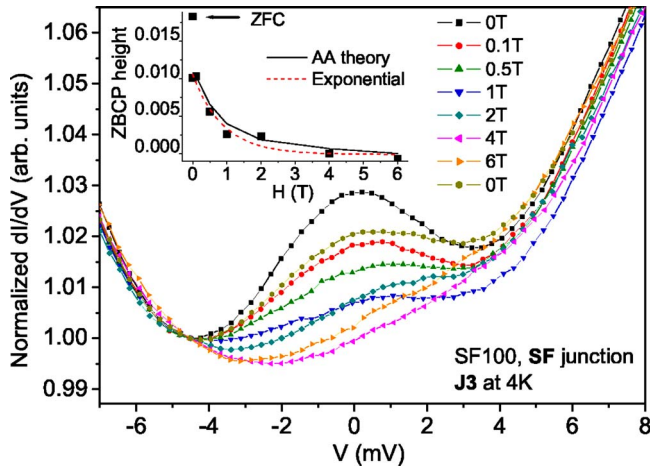


FIG. 6. (Color online) Normalized conductance spectra of an SF junction under ZFC to 4 K and various magnetic fields at low temperature. Inset: the ZBCP peak height $G_0 - G_B$ versus field. The curves are a typical Anderson-Appelbaum fit and an exponential fit.

should be higher than the conductance after field cycling. This is so since the magnetic memory after the field cycling reduces the number of domains as shown schematically in the lower-left corner of the inset to Fig. 5. Because this is exactly the observed result, we conclude that the CARE is responsible for the excess conductance at zero field under ZFC as shown in the inset to Fig. 5. We stress that this phenomenon is a unique signature of the CARE, which *cannot* be explained by the standard Andreev reflections.

Next, we decided to look at the limit of a very thick barrier. Since the Ohmic resistivity of SRO is quite small at 4 K, only $\sim 50 \mu\Omega \text{ cm}$ as shown in inset (a) of Fig. 1, we chose to study SF rather than SFS junctions. In this case, the F electrode “thickness” or size is almost infinite, and therefore its relatively weak itinerant ferromagnetism should be enhanced.⁷ The resulting conductance spectra of a typical SF junction are shown in Fig. 6. The spectra and the ZBCP height values versus field were obtained by ZFC to 4 K, ramping to 6 T, and going back to 0 T. The ZBCP inside a gaplike structure is still present, but its magnitude is greatly reduced compared to the previous data in SFS junctions. The interesting feature here is that already at 4 T, the ZBCP is almost fully suppressed. Under this field the SRO electrode is almost fully polarized and the disappearance of the ZBCP is in agreement with theoretical predictions.²⁶ Even more amazing is the field dependence of the ZBCP height as shown in the inset to Fig. 6. This is clearly *nonlinear* and rather close to exponential decay. Actually, this decay is very similar to that predicted by the Anderson-Appelbaum (AA) theory of scattering by magnetic states close to the interface with a superconductor.^{16,17,24} It should be noted that in the AA model this decay is due to the increased Zeeman splitting of the ZBCP.²³ We, however, had never observed splitting of the ZBCP, and this could be due to a larger magnetic relaxation rate in SRO which broadens this peak and smears the splitting. It is therefore concluded that the almost exponential decay versus field for fields higher than about 0.1 T indicates that the dominant transport mechanism is probably magnetic scattering. We conclude that the size of the F electrode plays

an important role in determining the transport properties of our junctions. When the F electrode is thin as in the previous results of SFS junctions (10–20 nm), its ferromagnetism is weak and the proximity effect by the S electrodes makes it even weaker. The opposite is true when the F electrode size is large as in the SF junctions case. Then the proximity penetration of superconductivity into F is small compared to the mean free path in the F electrode (which is unlimited now by the junction length), the ferromagnetic order in F is robust, and the transport in the junction is controlled mostly by magnetic scattering.

We note that the value of the ZBCP height after ZFC from room temperature to 4 K is still much larger than its value after field cycling to 6 T and back to 0 T, similar to the result in the SFS junction of Fig. 5. It is tempting to attribute this behavior to the CARE as before, but then the absence of a linear decreasing component of the ZBCP height versus field, which originates in Andreev scattering, will have to be explained. According to Yokoyama *et al.* who calculated the conductance spectra due to magnetic scattering in SN junctions with a d-wave superconductor,²⁷ an enhanced magnetic scattering rate (by the higher magnetic disorder after ZFC in the present study) would decrease rather than increase the ZBCP. Since this is opposite to observation, it seems that we are still dealing with suppression of the ZBCP height due to the CARE here (from the magnetically disordered ZFC state to the more ordered state after field cycling, similar to the result in Fig. 5). Apparently, in the SF case where the ferromagnetism of F is robust, the linear suppression of the ZBCP height versus field is much enhanced and terminates at a much smaller applied field of about 0.1–0.2 T. This leaves only the exponential decay versus field at higher fields due to magnetic scattering as the dominant process.

Finally, we compare our results to those obtained in YBCO-manganite SF junctions.^{28,29} These junctions were prepared with $\text{La}_{0.67}\text{Sr}_{0.33}\text{MnO}_3$ electrodes crossing over YBCO stripes. A magnetic field was applied in the *a-b* plane, and the conductance spectra were measured. A robust ZBCP was observed in these studies, which was hardly affected by a magnetic field of up to 14 T. This behavior is in clear disagreement with our results where the ZBCP decays with increasing field either linearly or exponentially. The reasons for this discrepancy could be the different F electrode materials, the different field orientations (ours was along the *c* axis), and the different preparation procedures (ours was fully dry with no acid etching). Furthermore, preliminary results in our type of SFS junctions with a different manganite $\text{Nd}_{0.67}\text{Sr}_{0.33}\text{MnO}_3$ barrier showed a strong ZBCP at 4 K which decayed almost exponentially with magnetic field. This result is also in contradiction to the results of Refs. 28 and 29, which calls for more studies of this issue.

In conclusion, we have found significant magnetic effects in the transport properties of SFS and SF junctions of YBCO and the SRO ferromagnet. (i) We observed an asymmetry in the conductance spectra and shifts of bound-state peaks with field, which are typical of magnetic tunneling junctions. (ii) In both types of junctions a prominent ZBCP was observed. Its height decreased linearly with increasing field in SFS junctions, but almost exponentially in the SF case. The ZBCP height dependence on *H* originated in normal Andreev

scattering and the CARE in the SFS junctions, but was dominated by magnetic scattering in the SF junctions. (iii) The observation of a higher ZBCP height at 0 T after ZFC as compared to the value after field cycling is due to the higher magnetic disorder after ZFC in both SFS and SF junctions. This is a strong signature of a CARE phenomenon in our junctions. Finally, we note that a calculation of the conductance spectra under fields in SF and SFS junctions is needed

for a more quantitative comparison with the present results.

The authors are grateful to G. Deutscher, L. Klein, O. Millo, and E. Polturak for useful discussions. This research was supported in part by the Israel Science Foundation (Grant No. 1564/04), the Heinrich Hertz Minerva Center for HTSC, and the Fund for the Promotion of Research at the Technion.

*Electronic address: gkoren@physics.technion.ac.il; URL: <http://physics.technion.ac.il/~gkoren>

- ¹L. Antognazza, K. Char, T. H. Geballe, L. L. King, and A. W. Sleight, *Appl. Phys. Lett.* **63**, 1005 (1993).
- ²R. Domel, C. Horstmann, M. Siegel, A. I. Braginski, and M. Yu. Kupriyanov, *Appl. Phys. Lett.* **67**, 1775 (1995).
- ³K. Char, L. Antognazza, and T. H. Geballe, *Appl. Phys. Lett.* **63**, 2420 (1993).
- ⁴E. Olsson and K. Char, *Appl. Phys. Lett.* **64**, 1292 (1994).
- ⁵L. Antognazza, K. Char, and T. H. Geballe, *Appl. Phys. Lett.* **68**, 1009 (1996).
- ⁶K. Char, M. S. Colclough, T. H. Geballe, and K. E. Myers, *Appl. Phys. Lett.* **62**, 196 (1993).
- ⁷L. Klein, J. S. Dodge, C. H. Ahn, J. W. Reiner, L. Mieville, T. H. Geballe, M. R. Beasley, and A. Kapitulnik, *J. Phys.: Condens. Matter* **8**, 10111 (1996).
- ⁸N. D. Zaharov, K. M. Satyalakshmi, G. Koren, and D. Hesse, *J. Mater. Res.* **14**, 4385 (1999).
- ⁹G. Deutscher and D. Feinberg, *Appl. Phys. Lett.* **76**, 487 (2000).
- ¹⁰A. F. Marshall, L. Klein, J. S. Dodge, C. H. Ahn, J. W. Reiner, L. Mieville, L. Antognazza, A. Kapitulnik, T. H. Geballe, and M. R. Beasley, *J. Appl. Phys.* **85**, 4131 (1999).
- ¹¹M. Feigensohn, L. Klein, J. W. Reiner, and M. R. Beasley, *Phys. Rev. B* **67**, 134436 (2003).
- ¹²D. Beckmann, H. B. Weber, and H. v. Löhneysen, *Phys. Rev. Lett.* **93**, 197003 (2004).
- ¹³O. Neshet and G. Koren, *Appl. Phys. Lett.* **74**, 3392 (1999).
- ¹⁴L. I. Glazman and K. A. Matveev, *Zh. Eksp. Teor. Fiz.* **94**, 332 (1988) [*Sov. Phys. JETP* **67**, 1276 (1988)].
- ¹⁵A. F. Andreev, *Zh. Eksp. Teor. Fiz.* **46**, 1823 (1964) [*Sov. Phys. JETP* **19**, 1228 (1964)].
- ¹⁶J. Appelbaum, *Phys. Rev. Lett.* **17**, 91 (1966).
- ¹⁷P. W. Anderson, *Phys. Rev. Lett.* **17**, 95 (1966).
- ¹⁸Y. Tanaka, H. Tsuchiura, Y. Tanuma, and S. Kashiwaya, *J. Phys. Soc. Jpn.* **71**, 271 (2002).
- ¹⁹Y. Tanaka, H. Itoh, H. Tsuchiura, Y. Tanuma, J. Inoue, and S. Kashiwaya, *Physica C* **367**, 73 (2002).
- ²⁰G. Koren and N. Levy, *Europhys. Lett.* **59**, 121 (2002); **59**, 634(E) (2002).
- ²¹Y. Tanuma, Y. Tanaka, M. Yamashiro, and S. Kashiwaya, *Phys. Rev. B* **57**, 7997 (1998).
- ²²P. M. Tedrow and R. Meservey, *Phys. Rev. B* **7**, 318 (1973).
- ²³J. A. Appelbaum, *Phys. Rev.* **154**, 633 (1967).
- ²⁴J. A. Appelbaum and L. Y. L. Shen, *Phys. Rev. B* **5**, 544 (1972).
- ²⁵T. Yamashita, S. Takahashi, and S. Maekawa, *Phys. Rev. B* **68**, 174504 (2003).
- ²⁶S. Kashiwaya, Y. Tanaka, N. Yoshida, and M. R. Beasley, *Phys. Rev. B* **60**, 3572 (1999).
- ²⁷T. Yokoyama, Y. Tanaka, A. A. Golubov, J. Inoue, and Y. Asano, *Phys. Rev. B* **71**, 094506 (2005).
- ²⁸A. Sawa, S. Kashiwaya, H. Obara, H. Yamasaki, M. Koyanagi, N. Yoshida, and Y. Tanaka, *Physica C* **339**, 287 (2000).
- ²⁹H. Kashiwaya, S. Kashiwaya, B. Prijamboedi, A. Sawa, I. Kurosawa, Y. Tanaka, and I. Iguchi, *Phys. Rev. B* **70**, 094501 (2004).